

## X-ray Microscopy Studies of Protein Adsorption on a Phase Segregated Polystyrene/Polymethylmethacrylate Surface. 2. Effect of pH on Site Preference

Li Li,<sup>†</sup> Adam P. Hitchcock,<sup>\*,†</sup> Rena Cornelius,<sup>‡</sup> John L. Brash,<sup>†,‡,§</sup> Andreas Scholl,<sup>||</sup> and Andrew Doran<sup>||</sup>

BIMR, McMaster University, Hamilton, Ontario L8S 4M1, Canada, Chemical Engineering, McMaster University, Hamilton, Ontario L8S 4L7, Canada, School of Biomedical Engineering, McMaster University, Hamilton, Ontario L8S 4K1, Canada, and Advanced Light Source, Berkeley Lab, Berkeley, California 94720

Received: August 15, 2007; In Final Form: December 3, 2007

X-ray photoemission electron microscopy (XPEEM) using synchrotron radiation illumination has been used to study the adsorption of human serum albumin (HSA) onto a phase segregated polystyrene/polymethylmethacrylate (PS/PMMA) blend surface from solutions of five different pH values. The absolute coverage of albumin on each of three chemically distinct components of the surface, PS domains, PMMA domains, and the interface between the domains, was determined from a quantitative analysis of C 1s image sequences. At all pH values, the preferred adsorption site is the interface. At neutral pH (7.0), albumin showed a slight preference for PS regions relative to PMMA. At strongly acidic pH (2.0) and strongly basic pH (10.0), similar amounts of albumin adsorb on the PS and PMMA regions. However, at pH 4.0, the amount of albumin adsorbed on PMMA domains is  $\sim 1.6$  times greater than that on PS domains, while at pH 8.6 the amount of albumin adsorbed on PMMA is one-half that adsorbed on PS domains. The pH dependence of the site preference is rationalized in terms of the known changes of albumin conformation with pH [Peters, T., Jr. *All About Albumin: Biochemistry, Genetics, and Medical Applications*; Academic Press: New York, 1995]. We infer from our results that the site preference of albumin adsorption on PS/PMMA blends is related mainly to changes in hydrophobic interactions, which are driven by pH-dependent electrostatic effects, that is, changes to the protein surface structure as the charge on the protein changes. The results provide insight into changes in the secondary structure of albumin in acid and basic media.

### 1. Introduction

Human serum albumin (HSA) has been used widely as a model protein to study the interactions between proteins and surfaces. It is the most abundant of the plasma proteins, and it is the major carrier of fatty acids in the blood.<sup>1</sup> HSA consists of 585 amino acids in a single polypeptide chain. The conformation of HSA in an aqueous environment depends on pH. Foster<sup>2</sup> has labeled five of these conformations E, F, N, B, and A and has suggested structures for the conformers, of which those for N, F, and E are shown in Figure 1. The protein consists of three homologous domains (I, II, and III), and each domain contains two subdomains. With decreasing pH, the compact “native” (N) albumin structure undergoes reversible conformational isomerization leading to unfolding of the molecule. The N–F transition involves unfolding of domain III. The F form is characterized by a dramatic increase in viscosity, much lower solubility, and a significant loss in  $\alpha$  helix content as compared to the N form. At pH lower than 4, the molecule undergoes additional expansion with additional loss of  $\alpha$  helix content. This expanded form, known as the E form, has increased intrinsic viscosity, and an increase in the hydrodynamic axial ratio from  $\sim 4$  to above 9. At pH's higher than 8, albumin undergoes contraction. At pH 8, albumin changes conformation

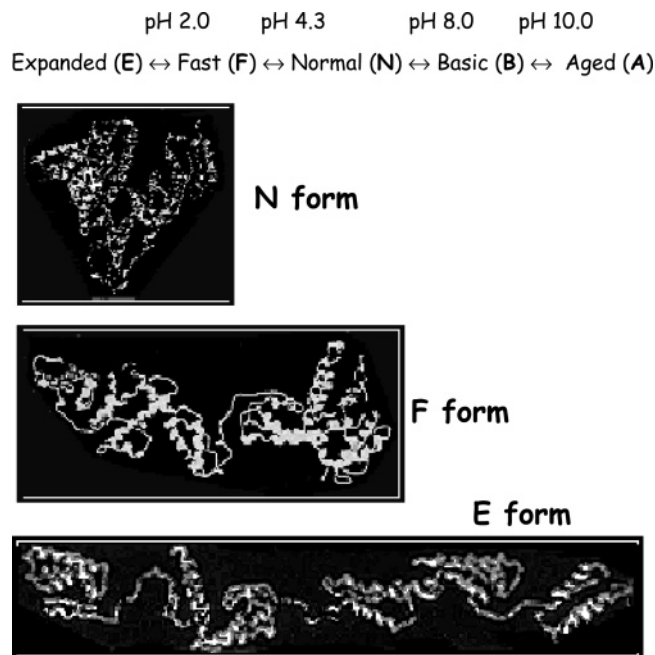


**Figure 1.** (a) Conformations of human serum albumin (HSA) at different pH (adapted from ref 2, with permission).

to the basic form (B). At pH above 10, another reversible isomerization occurs to create the A form. Details of the A and B form are given in ref 1. Structures for the F and E forms have been proposed by Carter et al.<sup>3</sup> Recently, Qiu et al.<sup>4</sup> used

\* To whom correspondence should be addressed. E-mail: aph@mcmaster.ca.

<sup>†</sup> BIMR, McMaster University.

<sup>‡</sup> Chemical Engineering, McMaster University.

<sup>§</sup> School of Biomedical Engineering, McMaster University.

<sup>||</sup> Berkeley Lab.

a single intrinsic tryptophan residue as a local molecular probe to study conformational changes in albumin at different pH using a femtosecond-resolved fluorescence method. They found that albumin is in a flexible state at neutral pH, an extended state at acidic pH, and a contracted state at basic pH. The isoelectric point of the protein is 4.7, and there are very large changes in the total surface charge and the surface charge distribution with pH,<sup>1</sup> which are probably a major driving force in conformational rearrangements.

This study is intended to contribute to better understanding of blood interactions with solid surfaces, an important consideration in the development of biomaterials for use in blood contacting medical devices. The initial interactions of a biomaterial surface with blood proteins are considered critical to biocompatibility. We are using X-ray photoemission electron microscopy (XPEEM) to study the adsorption of blood proteins onto polymer blend surfaces that have chemically distinct domains.<sup>5–7</sup> XPEEM has the capability to map adsorbed proteins at submonolayer coverage simultaneously with the surface components of the polymer substrate at high spatial resolution ( $\sim 80$  nm). Thus it is a unique and effective tool to explore the differential adsorption of proteins to chemically distinct regions of a heterogeneous surface in a single experiment. In a recent Article<sup>7</sup> (referred to hereinafter as **I**), the adsorption of albumin from deionized aqueous solutions on to a phase segregated polystyrene/polymethylmethacrylate (PS/PMMA) blend surface was studied by X-PEEM as a function of solution concentration and time. The methodology, typical results, and adsorption mechanism were discussed.

The work reported in the present Article extends these investigations and uses both X-PEEM and <sup>125</sup>I-radiolabeling to study the adsorption of albumin from aqueous solutions of different pH to this same PS/PMMA blend surface. We hypothesize that by varying the pH (and thus the protein conformation as described above), possible changes in the adsorption distributions would provide new insights into protein interfacial behavior on different types of polymer surfaces. From the measured distributions of albumin on chemically distinct regions of the surface (PS domains, PMMA domains, and the PS/PMMA domain interfaces), we were able to identify the relative site preferences for HSA adsorption from solutions of different pH. The change of adsorption site preference was found to be correlated with pH-dependent changes in overall conformation, charge, and the relative amounts of hydrophobic versus hydrophilic residues at the surface of the albumin. It is proposed that these conformational changes are due to the breaking or forming of hydrogen bonds as the albumin unfolds or contracts with change in pH. Recently, Sousa et al.<sup>8</sup> reported an electron microscopy study of the effect of pH on the site preference for adsorption of ferritin on a polycaprolactam/polycarbonate blend surface. We compare our results to that work.

## 2. Experimental Section

**2.1. Materials.** **2.1.1. PS/PMMA Substrate.** Full details of the preparation of native oxide silicon wafer substrates and the thin films of the PS/PMMA were presented in **I**.<sup>7</sup> Briefly, a 30:70 w/w PS/PMMA (1 wt %) toluene solution was spun cast (4000 rpm, 40 s) onto clean  $0.8 \times 0.8$  cm native oxide Si wafers (111). The PS (MW = 1.07 M,  $\delta$  = 1.06) and PMMA (MW = 312 K,  $\delta$  = 1.01) were obtained from Polymer Source and were used without further purification. The PS/PMMA covered Si substrates were annealed at 160 °C for 12 h in a vacuum oven at a pressure of  $\sim 10^{-4}$  Torr. This preparation produces a phase segregated surface (and bulk) with discrete ovoid PMMA

domains in a continuous domain of PS. Both the PS and the PMMA domains also contain microdomains at the 10–200 nm size scale, amounting to  $\sim 20\%$  of the area of the majority domain. Noncontact mode atomic force microscopy (AFM) measurements across a scratch through the polymer film showed the PS/PMMA film to be 40–50 nm thick with very low rugosity (2–3 nm rms).

**2.1.2. Protein Solutions.** Human serum albumin (HSA) was obtained from Behringwerke AG, Marburg, Germany, and found to be homogeneous as judged by sodium dodecyl sulfate polyacrylamide gel electrophoresis (SDS-PAGE). HSA solutions of 0.05 mg/mL concentration were diluted from the stock solutions (0.2 mg/mL) prepared at four different pH values. The neutral pH solution was prepared from unbuffered deionized water. Its pH was  $7.0 \pm 0.1$ . The pH 2.0 and pH 4.0 solutions were prepared by adding HCl dropwise to the unbuffered deionized water solution; the solutions of pH 8.6 and pH 10.0 were prepared by adding NaOH dropwise to the unbuffered deionized water solution.

**2.2. Experiments with Radiolabeled Proteins.** HSA was labeled with <sup>125</sup>I (ICN Biomedicals, Mississauga, ON, Canada) using the iodogen technique,<sup>9</sup> a standard protocol for radioiodination of proteins with IODO-GEN (Pierce Chemical Company, Rockford, IL).<sup>10</sup> The labeled protein was dialyzed overnight against isotonic Tris buffer to remove unbound radioactive iodide. Trichloroacetic acid precipitation<sup>11</sup> of aliquots of protein solutions before and after completion of the experiments confirmed that  $>99\%$  of the <sup>125</sup>I remained bound to the protein. The adsorption experiments were carried out under static conditions as described previously<sup>7</sup> at pH values of 2.0, 4.0, 7.0, 8.6, and 10.0. The albumin concentration used was fixed at 0.05 mg/mL with 10% labeled albumin, and the adsorption time was 20 min. After adsorption the surfaces were rinsed statically for 2.5 min using water at the same pH. Adsorbed amounts were calculated as described elsewhere.<sup>12</sup> Each adsorption experiment was performed in four replicates.

**2.3. Protein Exposure for XPEEM Study.** The protein adsorption method was the same as described in **I**.<sup>7</sup> Incubation of the PS/PMMA/Si substrate in albumin solutions of defined pH was performed in a Fisher multiwell plate (1 cm diameter wells). The incubation time for each sample was 20 min. After incubation, the samples were washed multiple times using water at the same pH.

**2.4. XPEEM Measurements.** The XPEEM at the ALS bending magnet beamline 7.3.1<sup>13</sup> was used for this work. The experimental conditions were the same as described previously.<sup>7</sup> Image sequences (stacks<sup>14</sup>) in the C 1s edge region (282–293 eV) were recorded from several different areas of each sample. These C 1s image sequences were analyzed to generate quantitative maps of the PS, PMMA, and protein distributions using quantitative C 1s reference spectra of albumin, PS, and PMMA, which were reported in **I**.<sup>7</sup> In principle, the C 1s spectrum of albumin might change with changes in pH, although such changes are expected to be small because X-ray absorption spectra are not sensitive to long-range order, which is the main effect of pH changes (see Figure 1). The C 1s spectrum of HSA was measured at pH = 4 and pH = 10 (not shown), and the spectra were the same as at neutral pH.

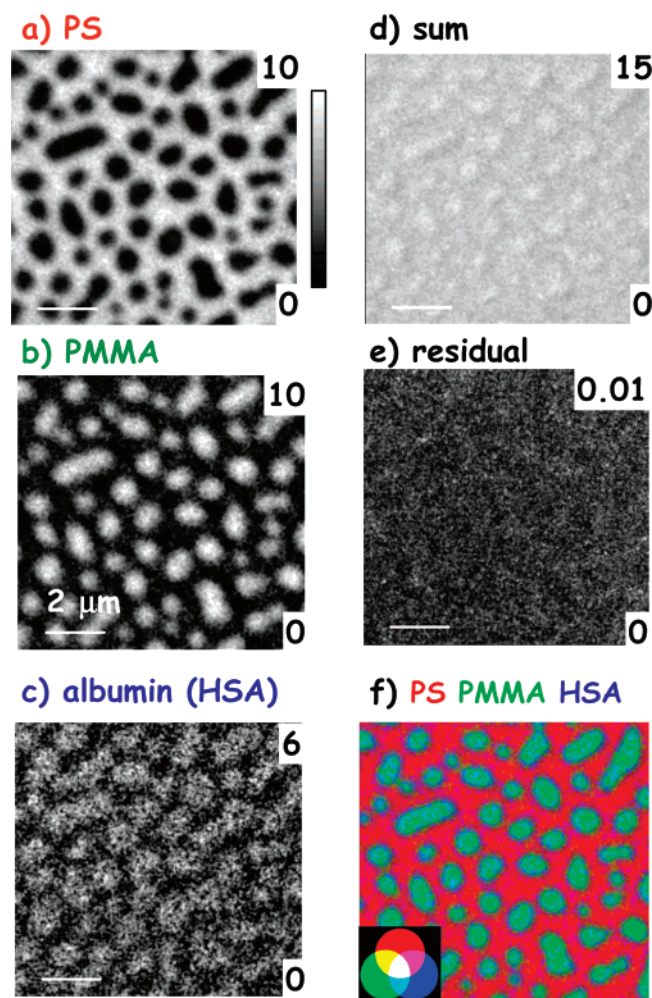
## 3. Results

**3.1. Adsorption of HSA from <sup>125</sup>I-Labeling Experiments.** Table 1 shows data on the adsorption of <sup>125</sup>I-labeled HSA to the PS/PMMA blend surface at different values of pH. The highest adsorption occurred at pH 4.0 close to the isoelectric



**TABLE 1: Adsorption of Albumin on the PS/PMMA Surface at Different pH Values Determined by  $^{125}\text{I}$ -Radiolabeling Experiments (Data Are in  $\mu\text{g}/\text{cm}^2$ )**

	pH 2.0	pH 4.0	pH 7.0	pH 8.6	pH 10.0
adsorbed quantity	0.117(3) <sup>a</sup>	0.223(2)	0.14(2)	0.13(2)	0.138(3)

<sup>a</sup> Standard deviation,  $n = 4$ .

**Figure 2.** Component maps of (a) PS, (b) PMMA, and (c) albumin for a PS/PMMA blend substrate exposed for 20 min to a 0.05 mg/mL aqueous solution of HSA at pH 4, derived from pixel-by-pixel curve fits of a C 1s image sequence. The numbers in the upper and lower right of each component map are the minimum and maximum thicknesses (in nm) for the gray scales. (d) Sum of the PS, PMMA, and albumin thickness component maps. (e) Map of the residual of the fit. The gray scale in this case is the deviation of the fit and the measured signal, averaged over all energies. (f) False color composite of the three component maps (red = PS, green = PMMA, blue = albumin) using independent rescaling of each component.

point ( $pI = 4.7$ ) where, typically, protein adsorption has been observed to be at a maximum.<sup>15,16</sup> At the other four pH values studied, the amount adsorbed was similar and about a factor of 2 smaller than at pH 4.0.

**3.2. Regional Distribution of Adsorbed HSA from XPEEM Measurements.** Because the data sets used in this work are different from those in ref 7 and a new way of presenting the results is introduced, an example of the mapping and curve fit analysis is presented. Figure 2 displays the results from analysis of a C 1s stack recorded from a PS/PMMA surface exposed to a 0.05 mg/mL HSA solution at pH = 4.0. The figure presents quantitative maps of each component: (a) PS, (b) PMMA, (c)

albumin, as well as (d) the sum of these components, (e) the residual of the fit, and (f) a false color composite map. The component maps are constructed from the coefficients obtained from curve fits of the spectrum at each pixel to a linear combination of the reference spectra for the three components (PS, PMMA, HSA) and an additional “constant” (energy-independent) term using the “stack fit” procedure.<sup>17</sup> The relative amounts of each component at each pixel are made absolute (in terms of thickness of that component contributing to the overall signal) by scaling with a factor determined by setting the sum of all three component map signals to the estimated total sampling depth of 10 nm,<sup>18</sup> as described in detail in ref 7. Consequently, each component map is the spatial distribution of that component with the quantity at each pixel represented by its shade on the gray scale, for which the limits are indicated by the numbers at the lower right (minimum) and upper right (maximum) of each map. Lighter intensities indicate locations where there is more of that component. Note that at each of the pH conditions in this work the summed signal was constant within 15% over the whole field of view, supporting the underlying assumption that the total sampling depth, measured for PS to be 10 nm,<sup>18</sup> is similar in the chemically different regions.

The component maps of PS, PMMA, and albumin can be combined to form a false color composite map, which reveals the spatial correlation of the chemical components, as shown in Figure 2f. The PS signal is mapped to red, the PMMA to green, and the albumin to blue, with the full scale of each color mapped to the gray scale limits of each component (rescaled mapping). The maps show the variation in the spatial distributions of the protein on the various chemically different parts of the surface. The “purer” is the red (or green) color, the smaller is the amount of protein that is present on the PS (or PMMA) domains. The bluish-purple color of the continuous PS domains indicates a significant amount of protein on these domains. In this case, the false color map shows a distinct blue band at the interface between the PS and PMMA domains, indicating a preference for albumin adsorption at the PS/PMMA interfaces at pH 4.0. A similar analysis procedure was applied to C 1s image sequence data measured for surfaces prepared at each of the five pH values studied.

Figure 3 presents false color composite maps derived from stack fits of C 1s image sequences measured for adsorption at pH values of 2.0, 4.0, 7.0, 8.6, and 10.0, derived using the same procedure as described for pH 4.0. The presence of distinct blue color in the PS/PMMA interface regions shows that albumin adsorbs preferentially to the PS/PMMA interfaces at all of the pH conditions examined.

To obtain the quantities of albumin on the different domains, the domains were first identified by applying a threshold procedure to the component maps to generate a binary mask consisting of those pixels where the PS (or PMMA) signal was above a defined threshold. The signal from an  $\sim 80$  nm wide band at the PS–PMMA interface (taken as the interface domain) was obtained by selecting those pixels not present in either the PS-domain or the PMMA-domain masks. The amount of each component (PS, PMMA, and albumin) in each domain (PS, PMMA, interface) was then obtained by extracting the spectrum integrated over each mask (PS, PMMA, interface) and fitting that extracted spectrum using the same reference spectra. Figure 4 shows this procedure for the case of the pH 4.0 data set. Panel a shows the PS, PMMA, and interface masks in a single false color display. Panels b–d show the spectra extracted from each area along with the curve fit. The points with estimated

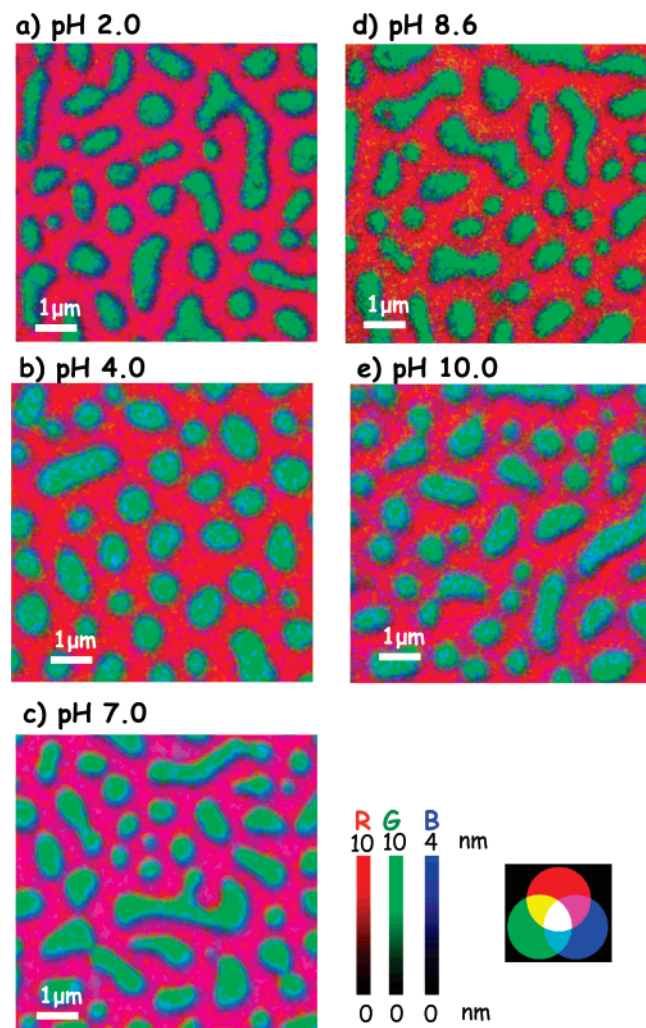


**Figure 3.** Rescaled false color composites of component maps (red = PS, green = PMMA, blue = albumin) of albumin covered PS/PMMA derived from C 1s image sequences recorded for albumin on PS/PMMA prepared using the five different pH's. The data for each pH value were analyzed and the composites were prepared as described in Figure 2.

uncertainties are the experimental spectra; the thicker curves are the fits to the experimental spectra of each masked region, and the thinner (colored) curves are the weighted reference spectra. The results of the curve fits to the extracted spectra for each of the five pH data sets are reported in Table 2.

A complication of this analysis is the fact that there is incomplete phase segregation of the PS/PMMA blend due to limited mobility associated with the high molecular weights.<sup>5</sup> In this case, about 10–20% PMMA is present in the masked PS region in the form of unresolved or partly resolved 50–200 nm diameter microdomains of PMMA and about 20–25% PS is present as microdomains in the masked PMMA region. The interfacial region contains about equal amounts of PS and PMMA, as expected. Despite the incomplete phase separation, it is nonetheless clear that there are adsorption preferences with respect to the three chemically different regions. The amounts of albumin on these chemically different regions are highlighted in bold in Table 2. The last row of the table shows the ratios of the amounts of albumin on each of the three different regions.

As seen in both the false color maps and the numerical results from the curve fit, there is a preference for albumin to adsorb at the PS/PMMA interface at all pH conditions. At neutral pH (7.0), albumin shows a slightly stronger preference for the PS

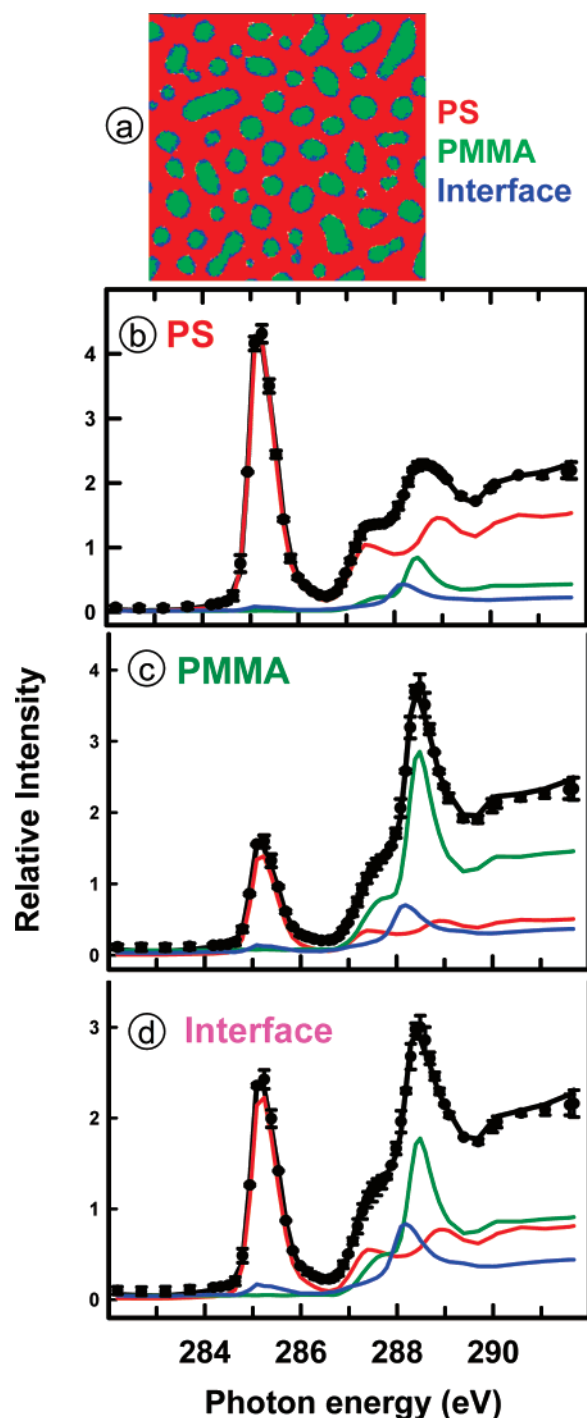


**Figure 4.** (a) Mask used to extract spectra of specific regions from the pH = 4.0 data. Red = PS > 4 nm, green = PMMA > 4 nm, blue = PS/PMMA interface (all pixels not identified in the masks of the PS and PMMA domains). (b–d) Curve fits to the average C 1s spectra extracted from the masked regions (data, dots; fit, thick solid line; components, thin lines).

relative to the PMMA domains. At strongly acidic pH (2.0) and strongly basic pH (10) values, similar amounts of albumin are adsorbed on the PS and PMMA domains. However, at moderately acidic (4.0) and basic pH (8.6), albumin shows distinctly different adsorption behavior. At pH 4.0, adsorption on the PMMA domains is ~1.6 times greater than that on the PS domains (PMMA preference), while at pH 8.6 adsorption on PMMA is about one-half of that on the PS domains (PS preference). Selective adsorption of protein to heterogeneous polymer surfaces has been documented elsewhere,<sup>6,7,19</sup> including



**TABLE 2: Thickness of Albumin (nm/pixel) on the PS and PMMA Domains and at the PS/PMMA Interface as a Function of pH (Uncertainty:  $\pm 0.1$  nm)**

region <sup>a</sup>	component	thickness (nm/pixel)				
		pH 2.0	pH 4.0	pH 7.0	pH 8.6	pH 10.0
PS	PS	5.8	6.9	5.8	7.2	6.3
	PMMA	1.7	1.7	1.6	2.0	1.8
	albumin	<b>2.5</b>	<b>1.4</b>	<b>2.6</b>	<b>0.8</b>	<b>1.9</b>
PMMA	PS	1.8	2.1	2.3	2.4	2.5
	PMMA	5.9	5.6	5.6	7.2	5.3
	albumin	<b>2.3</b>	<b>2.3</b>	<b>2.1</b>	<b>0.4</b>	<b>2.2</b>
interface	PS	2.7	3.6	3.7	3.7	3.7
	PMMA	2.7	3.6	3.5	3.7	3.6
	albumin	<b>3.6</b>	<b>2.8</b>	<b>2.8</b>	<b>2.6</b>	<b>2.7</b>
albumin ratios: PS/PMMA/interface <sup>b</sup>		1.1/1.0/1.6	0.6/1.0/1.2	1.2/1.0/1.3	2.0/1.0/6.5	0.9/1.0/1.2

<sup>a</sup> The thickness threshold values from the component maps used for determining the pixels to include in this analysis were: PS, 4.5 nm/pixel; PMMA, 4.0 nm/pixel. The interface pixels are defined as those not present in the PS or PMMA domains. This constitutes a  $\sim 80$  nm wide band around each of the discrete PMMA domains. The pixel size used for the measurements was  $30 \text{ nm} \times 30 \text{ nm}$ . <sup>b</sup> Normalized so that value on PMMA domains is 1.0.

**TABLE 3: Average Thickness of Albumin (nm/pixel) on PS/PMMA Surface at Different pH Values Determined by XPEEM**

region		pH				
		2.0	4.0	7.0	8.6	10.0
PS	thickness	2.5	1.4	2.6	0.8	1.9
	% area	65	67	59	59	67
PMMA	thickness	2.3	2.3	2.1	0.4	2.2
	% area	27	24	33	27	24
interface	thickness	3.6	2.8	2.8	2.6	2.7
	% area	8	9	7	14	9
	average	2.5	1.7	2.4	1.0	2.0
	thickness <sup>a</sup>					

<sup>a</sup> Calculated using the formula:  $[\sum(\text{thickness} \times \% \text{ area})]/100$  for three regions.

a study by transmission electron microscopy of the effect of pH on the adsorption of ferritin to a blend of polycaprolactone and polycarbonate.<sup>8</sup> A detailed comparison of our results to those of Sousa et al.<sup>8</sup> is given in the Discussion.

The percentage of surface area for each region (PS, PMMA, or interface) is determined from the number of pixels in each region. The quantity of albumin on the surface as a whole (nm/pixel) is estimated by summing the products of the quantity on each region times the area of each region. Table 3 presents the average amount of adsorbed albumin on each region, along with the percentage of surface area and albumin thickness on each region for each pH. The XPEEM results indicate that the greatest amount of albumin was adsorbed at pH 2.0 and the smallest amount at pH 8.6.

**3.3. Visualizing the Surface Distribution of HAS.** False color maps of the albumin on the different regions of the surface (PS, PMMA, interface) were derived by first generating a mask to define each region as explained above (the threshold signal levels are given in Table 2; see Figure 4a for an example of the masks). The product of the mask of each region (e.g.,  $\text{PS}_{\text{mask}}$ ) and the albumin composition map (alb) is the map for the albumin distribution on that region (e.g.,  $\text{PS}_{\text{mask}} \times \text{alb} = \text{alb-on-PS}$ ; similarly for alb-on-PMMA, and alb-on-interface). For example, the alb-on-PS signal is generated by multiplying the albumin component map (see Figure 2c) and the masked map of PS regions (red region in Figure 4a). These three subcomponents of the total albumin map can then be recombined using false coloring to provide more insight into how albumin interacts with the PS/PMMA surface.

Figure 5 depicts the adsorbed albumin distributions on the three different regions as a function of pH. Each false color map is the combination of three component maps: the map of albumin on PS regions (alb-on-PS) in red, the map of albumin on PMMA regions (alb-on-PMMA) in green, and the map of

albumin on PS/PMMA interfaces (alb-on-interface) in blue. In the false color albumin distribution map, pure red on the PS regions indicates that the area is uniformly covered with adsorbed albumin, pure green on the PMMA regions indicates the area is uniformly covered with adsorbed albumin, and pure blue on the PS/PMMA interfaces indicates the area is uniformly covered with adsorbed albumin. Black pixels are locations with little or no adsorbed albumin. A common intensity scale, corresponding to a range of albumin thickness from 0 to 5 nm/pixel, is used for each map. The maps in Figure 5 show only a portion of the maps displayed in Figure 3 for a clearer view. For albumin adsorbed on the PS regions, the distribution is relatively uniform at all pH values except pH 4.0 and pH 10.0, where much of the adsorbed protein is near the edges of the PS regions. On the PMMA regions, albumin is adsorbed near the edges of the domains at pH 7.0 and 8.6, while the distribution is random for other pH values.

## 4. Discussion

**4.1. Comparison of <sup>125</sup>I-Radiolabeling and XPEEM Results.** Figure 6 compares the total quantity of HSA adsorbed to the PS/PMMA blend surfaces at different pH values, as measured by the two techniques. Clearly the pH dependence of the adsorbed amount is different for the two techniques. Two factors may be considered as possible explanations for the observed differences.

First, the intensity scale of the albumin reference spectrum is the response of 1 nm of albumin assuming a density of 1.0 mg/mL. If the albumin density changes with pH, the thickness will be overestimated for cases of increased density and underestimated for cases of decreased density. Kadi et al.<sup>20</sup> have reported that the partial specific volume of albumin increases from 0.737 to  $0.743 \times 10^{-3} \text{ m}^3/\text{kg}$  from pH 7.0 to pH 5.0, and

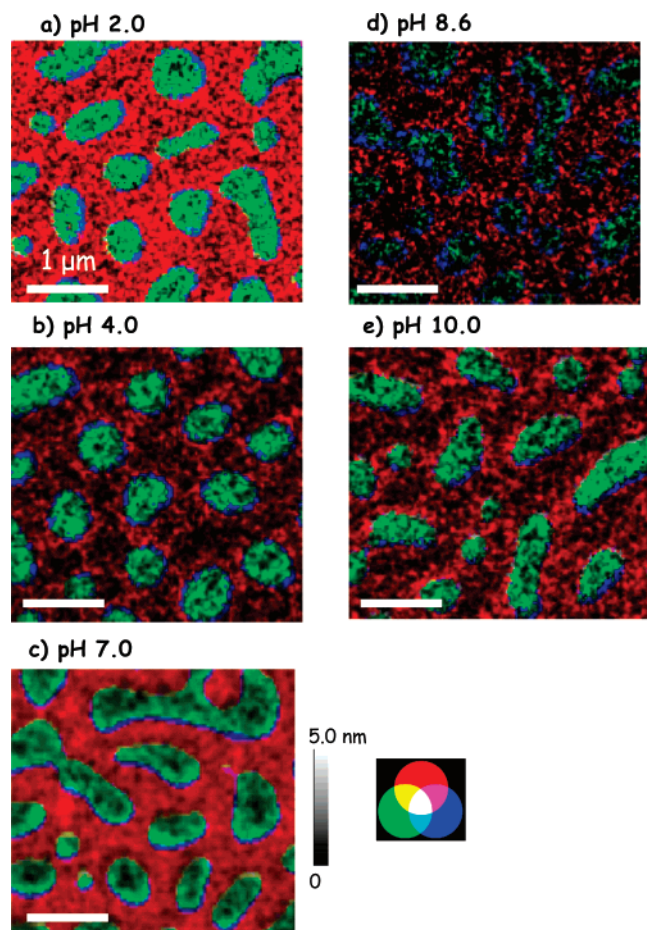


**Figure 5.** False color maps of the albumin distribution at each of the five pH values studied. The intensity of each color corresponds to the amount of albumin on the PS (red), PMMA (green), and interface (blue) regions, in all cases plotted on a color scale where brightest = 5.0 nm and darkest = 0 nm of adsorbed albumin.

then decreases to  $0.728 \times 10^{-3} \text{ m}^3/\text{kg}$  at pH 2–3.<sup>21</sup> The change in albumin density with pH is thus very small, so this is not likely to be the reason for the discrepancy in adsorbed amounts between the two techniques.

Second, XPEEM and radiolabeling measure different aspects of the adsorbed protein. The radiolabeling technique gives the number of HSA molecules adsorbed per unit surface area averaged over the entire surface, whereas XPEEM gives the thickness of the adsorbed protein per unit surface area, with the constraint that the maximum sampling depth is 10 nm and the decrease of sensitivity with depth is exponential.<sup>18</sup> The relationship between these two measures will depend on how the protein is oriented on the surface. At submonolayer or monolayer coverage (as in this work), if a protein with a dimension longer than 10 nm orients with its long axis perpendicular, XPEEM will underestimate the amount of protein because some protein signal will be lost due to the limited sampling depth of the method. If the orientation and size of the protein at submonolayer coverage is such that the layer thickness is less than 10 nm, there will be no loss of signal. Because of conformational changes, as summarized in the Introduction, the size and shape of albumin change with pH. Carter et al.<sup>21</sup> and Sugio et al.<sup>22</sup> have reported the three-dimensional crystal structure of HSA, which indicates that it is “heart-shaped” in the crystalline state with dimensions of  $3 \times 8 \times 8 \text{ nm}$ . By contrast, in solution at neutral pH albumin is reported to be a prolate ellipsoid with dimensions of  $4 \times 4 \times 14 \text{ nm}$ , based largely on hydrodynamic experiments,<sup>23–25</sup> and low-angle X-ray

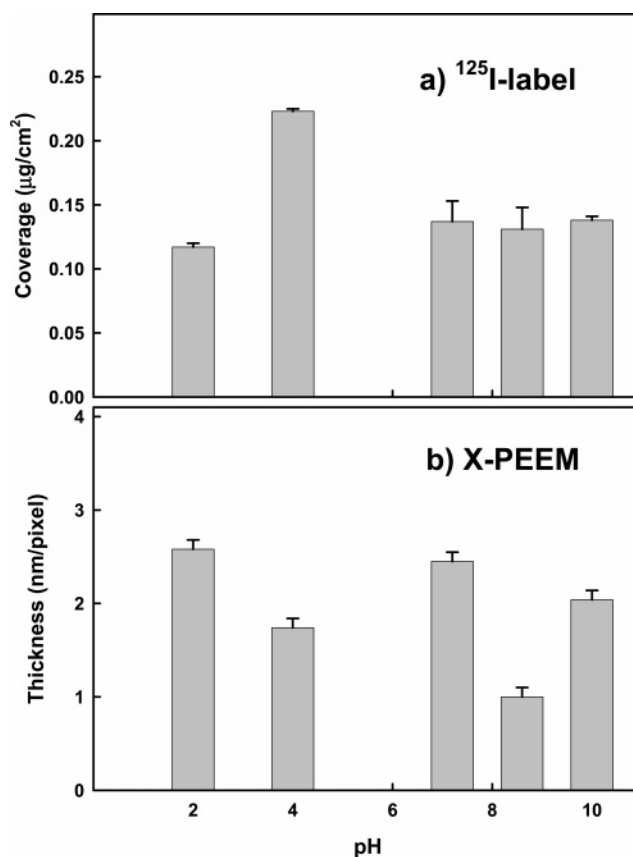


**Figure 6.** Comparison, as a function of pH, of (a) amount of adsorbed albumin ( $\mu\text{g}/\text{cm}^2$ ) on the PS/PMMA substrate derived from  $^{125}\text{I}$ -radiolabeling measurements with (b) thickness (nm/pixel, averaged over all chemical domains) derived from XPEEM.

scattering.<sup>26</sup> However, Ferrer et al.<sup>27</sup> have suggested that the albumin structure in solution at neutral pH is similar to that in the crystal and that the proposed prolate ellipsoid structure is incorrect. The F-form of albumin, which exists at pH 4.6, is reported to have a compact structure with dimensions of either  $2.1 \times 5 \times 10.6$  or  $2.7 \times 6.3 \times 8.2 \text{ nm}$ .<sup>28</sup> Electron microscopy images indicate that albumin in the E form (pH < 3) can be modeled as a set of balls and strings with overall dimensions of  $2.1 \times 2.1 \times 25 \text{ nm}$ .<sup>29</sup> More recently, Olivieri et al.<sup>30</sup> found that the molecular radius of gyration of albumin in solution ranges from 0.35 to 2.67 nm over the pH range from 7.0 to 2.5, but no molecular dimensions were reported. We are unaware of any data on the structure of albumin at basic pH (B and A forms).

Because albumin adopts different conformations at each of the five pH values studied, its size and shape will vary with pH. In addition, the adsorbed protein may orient on the surface in different ways at different pH. At neutral pH, surface plasmon resonance studies of albumin adsorption from a neutral solution onto a polystyrene surface<sup>31</sup> suggest that the preferred adsorption geometry is one with the albumin molecules oriented with their long axis parallel to the surface. If this were so, we would expect good correspondence between XPEEM and radiolabeling data at pH 7.0.

By assuming the adsorbed albumin has the same dimensions as in solution, the adsorbed quantity as measured by radiolabeling methods can be converted to thickness averaged over the surface ( $T$ ) according to eq 1:

$$T = \frac{V_{\text{alb}} \cdot \Gamma_{\text{radio}}}{a} \quad (1)$$

**TABLE 4: Calculated Average Thickness of Albumin (nm/pixel) on the Surface of PS/PMMA Blend Based on Adsorption Data from Radiolabeling Measurements (See Table 1)**

	pH				
	2.0	4.0	7.0	8.6	10.0
adsorption (radiolabeling) ( $\mu\text{g}/\text{cm}^2$ )	0.117	0.223	0.140	0.130	0.138
dimensions (nm)	$2.1 \times 2.1 \times 25$	$2.1 \times 5 \times 10.6$	$2.7 \times 6.3 \times 8.2$	$3 \times 8 \times 8$	$4 \times 4 \times 14$
[ref]	[29]	[28]	[27]	[21]	[24]
volume ( $\text{nm}^3$ )	110	111	139	192	224
calculated thickness <sup>a</sup>	1.1	2.2	2.8	2.4	1.2
calculated thickness <sup>b</sup>	1.0	1.9	2.4	2.4	1.0
XPEEM thickness	2.5	1.7	2.4	1.0	2.0

<sup>a</sup> Calculated using the normalizing factor  $a_1 = 11.2$ , assuming albumin dimensions of  $3 \times 8 \times 8 \text{ nm}^3$  at pH 7.0.<sup>21,22</sup> <sup>b</sup> Calculated using the normalizing factor  $a_2 = 13.1$ , assuming albumin dimensions of  $4 \times 4 \times 14 \text{ nm}^3$  at pH 7.0.<sup>23–26</sup> <sup>c</sup> The albumin volumes were estimated using eq 1 and assigning the XPEEM detected thickness equal to the calculated thicknesses.

where  $V_{\text{alb}}$  is the volume of the albumin molecule determined using the reported dimensions and approximating as a parallelepiped;  $\Gamma_{\text{radio}}$  is the mass per unit area as determined by the radiolabeling measurements; and  $a$  is a normalization constant. The dimensions of albumin at neutral pH<sup>23–26</sup> have been used as a “model” to calculate the normalization factor  $a$  (eq 2):

$$a = \left( \frac{V_{\text{alb}} \cdot \Gamma_{\text{radio}}}{T_{\text{XPEEM}}}_{\text{pH}7.0} \right) \quad (2)$$

This normalization factor can then be used to calculate the albumin thickness at other pH values according to eq 1. Several different values for the dimensions of albumin in neutral solution have been reported; therefore, the value of  $a$  depends on the dimensions chosen. For dimensions of  $3 \times 8 \times 8 \text{ nm}$ ,<sup>21</sup>  $a = 11.2$ ; for dimensions of  $4 \times 4 \times 14 \text{ nm}$ ,<sup>23–26</sup>  $a = 13.1$ .

The albumin thickness values calculated from the radiolabeling data using these equations are listed in Table 4 and are compared to the thickness measured by XPEEM. At pH 4.0, the thickness from the radiolabeling data is close to that from XPEEM when the protein dimensions are assumed to be  $2.1 \times 5 \times 10.6 \text{ nm}$ . In general, the thickness values derived from radiolabeling and XPEEM are in good agreement. At pH 2, however, the radiolabeling thickness is lower by a factor of 2 than the X-PEEM. This is a reproducible result for which we do not have an explanation at the present time.

The lack of data on the dimensions of albumin at pH 8.6 and 10.0 prevents the conversion of adsorbed quantity to thickness. As an alternative approach, the dimensions at these two pH values can be estimated by assigning the thickness values from XPEEM measurements. These numbers are listed in Table 4. From this evaluation, the albumin molecule appears to be similar in size at pH values of 2.0, 4.0, and 8.6, but smaller than at neutral pH. At pH 10.0, the molecule is similar in size to that at neutral pH.

**4.2. Regional Distribution of Albumin Adsorption.** As shown in Figure 5, the distributions of albumin on the PS and PMMA regions of the PS/PMMA blend surface are random and uniform at pH 2.0. At pH 4.0 and 10.0, albumin is adsorbed on the PS regions preferentially toward the interfaces (PS-edge preference), but the distribution on the PMMA regions is random. In contrast, at pH 7.0 and 8.6, albumin is adsorbed randomly on the PS regions but preferentially at the edges on the PMMA regions (PMMA-edge preference). The difference in the albumin distribution pattern at different pH values could be due to the conformational changes that occur with change

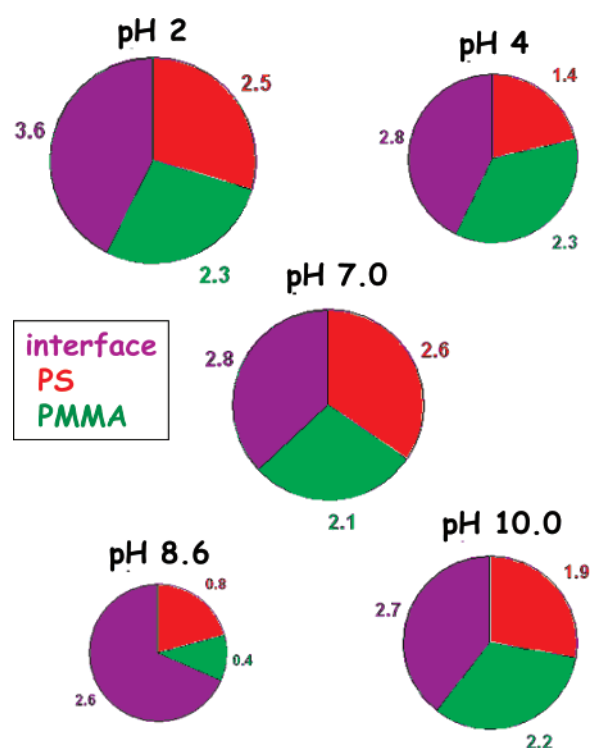


**Figure 7.** Relative amounts of albumin adsorbed on different regions as a function of pH (red = PS, green = PMMA, purple = interface) determined by XPEEM. The numbers are the average thickness (nm) on each region. The area of each circle is proportional to the total albumin on the surface at that pH, determined by XPEEM.

of pH. At pH 2.0, albumin is believed to be extensively unfolded and all sites on the outer envelope of the protein are equally accessible for adsorption; thus a random/uniform adsorption pattern would be expected over the surface as a whole. At the other pH values, albumin adopts a relatively compact structure in which certain sites are “hidden”. The changes in the nature of the protein surface may explain the different adsorption patterns observed on the PS and PMMA regions.

Figure 7 shows the regional distributions and total amounts of adsorbed albumin, as derived from X-PEEM, in the form of pie charts. The total area of each chart is proportional to the total amount of adsorbed albumin over the whole surface, while the relative amounts on the PS, PMMA, and PS/PMMA interface regions are indicated by the areas of the sections, which are scaled to be proportional to the albumin thickness (nm/pixel)



on each region. As the relative area of the purple (interface) wedges indicates, the PS/PMMA interface is the preferred adsorption site at all values of pH studied. The relative proportions adsorbed on the PS (red wedges) and PMMA (green wedges) regions are similar at pH values of 7.0, 2.0, and 10.0. However, at pH 4.0, PMMA is preferred over PS, while at pH 8.6, PS is preferred over PMMA.

The interface preference that dominates the adsorption site distribution at all values of pH has been explained<sup>7</sup> in terms of the combination of entropic contributions associated with hydrophobic interactions between the hydrophobic regions of HSA and PS and enthalpic contributions arising from hydrogen bonding between HSA and PMMA. To explain the pH dependence of the albumin distribution on the PS and PMMA regions, the surface properties of the PS/PMMA blend need to be considered. Polymer surfaces without formal charges usually have low surface charge density. The PS and PMMA polymers studied in this work should have zero surface charge because they were prepared by living anionic polymerization, and the introduction of any charged surface active materials was carefully avoided in sample preparation. The net charge on albumin varies with pH. At the isoelectric point ( $pI = 4.7$ ) the molecule has zero net charge. At pH 2.0, 4.0, 7.0, 8.6, and 10.0, the net charge is  $> +20$ ,  $+10$ ,  $-15$ ,  $-22$ , and  $-27$ , respectively.<sup>32</sup>

Despite the large change in net charge with pH, electrostatic interactions are not likely to be the dominant driving force for protein adsorption in these systems because PS and PMMA are uncharged. However, the charge on the protein at different pH values has an influence on its conformation. It appears that structural changes as a function of  $pH^{2-4}$  may explain the differences in adsorption preference at different pH values. Albumin undergoes contraction<sup>4</sup> as the pH increases from 7.0 to 10.0. The data presented here show similar adsorption of albumin to the PS and PMMA regions at pH 7.0 and 10.0, but a preference for PS over PMMA at pH 8.6. We interpret this to indicate that albumin has similar proportions of exposed hydrophobic and hydrophilic residues at pH 7.0 and pH 10.0. However, in the course of contraction, possibly driven by internal hydrogen bonding, the fraction of hydrophobic residues at the surface of the contracted albumin at pH 8.6 becomes relatively large. The more hydrophobic albumin surface at pH 8.6 would then result in an adsorption preference for PS. This interpretation is supported by a recent report showing that albumin is more hydrophobic at pH 9 (and presumably also at pH 10) than at pH 7.<sup>33</sup>

Albumin has been shown to undergo expansion (unfolding) as the pH decreases from 7.0 to 2.0.<sup>2,3</sup> The data presented here show similar adsorption of albumin to the PS and PMMA regions at pH 7.0 and 2.0, but a preference for PMMA over PS at pH 4.0. These results suggest that albumin may expose similar amounts of hydrophobic and hydrophilic residues at pH 7.0 and pH 2.0, but at pH 4.0, at an intermediate stage of expansion (unfolding), more hydrophilic than hydrophobic residues are exposed. The lower hydrophobicity of the albumin surface at pH 4.0 may then result in preferential adsorption to the PMMA regions over the PS. This is consistent with the findings of Alizadeh-Pasdar et al.<sup>33</sup> that the hydrophobicity of albumin is lower at pH 4.0 than at pH 7.0. In addition, Kadi et al.<sup>20</sup> proposed that albumin "buries" aromatic residues in a hydrophobic pocket by expulsion of water in contact with the aromatic residue when the pH changes from 7.0 to 4.0. Such a conformational change would result in a less hydrophobic albumin surface at pH 4.0.

By analogy with the suggestion that hydrophilic residues are "hidden" when albumin contracts in basic media, we propose that when albumin is partly unfolded at pH 4.0 it exposes hydrophilic residues by breaking hydrogen bonds, and consequently more hydrophobic residues are buried internally. We note that the surface hydrophobicity of a protein is generally measured using fluorescence probes or calculated from the known three-dimensional protein structure. The present work suggests that the surface hydrophobicity of a protein could be estimated by quantifying the distribution of adsorbed amount on a "standard" patterned surface consisting of domains of differing hydrophobic character.

It is interesting to compare our results and interpretation to those of Sousa et al.<sup>8</sup> who studied ferritin adsorption on a polycaprolactam (PCL)/polycarbonate (PDTD) blend surface. They reported a 3-fold preference for adsorption of ferritin on PDTD over PCL at physiological pH. However, when the pH was lowered to 3.5, below the isoelectric point of ferritin, there was little or no adsorption preference. Because ferritin is highly resistant to denaturation, only ionizable sites on the surface of the protein are involved. At pH 7.4, both the PCL and the ferritin are negatively charged, and thus the selectivity toward PDTD is actually due to electrostatic repulsion between PCL and ferritin. At pH 3.5, the ferritin becomes positively charged and is then able to adsorb to the negatively charged PCL as well as to PDTD, resulting in loss of selectivity. Thus the pH dependence of the adsorption selectivity in that case seems to be a purely electrostatic effect. In the PS/PMMA system, there is no charge at the surface of the polymer, and thus electrostatic interactions are likely to play a smaller role, although they must be an important driving force in the conformational changes with pH. Rather, PS and PMMA differ primarily in their ability to form hydrogen bonds or to experience van der Waals interactions with a protein. Because albumin is well known to undergo major conformational changes with pH, which will change the amounts of hydrophobic and hydrophilic regions exposed at the protein surface, we propose that it is hydrophobic interactions rather than any direct electrostatic effect that explains the pH dependence of the adsorption selectivity in the case of albumin adsorption on PS/PMMA blend surfaces.

## 5. Summary

The total adsorbed amounts (in terms of thickness per unit area) and the surface distribution of albumin on a phase segregated PS/PMMA blend surface at pH values between 2 and 10 were measured using XPEEM. Total adsorbed amounts were also measured by <sup>125</sup>I-radiolabeling methods. The XPEEM and radiolabel data on thickness were generally in agreement, except at pH 4.0 and 8.6 where the XPEEM data were significantly lower, for reasons that are not presently understood. The mapping of the albumin distributions by XPEEM revealed significant differences in adsorbed amounts and regional distributions at different pH values. The most striking effect is a strong preference for the PS-PMMA interface, which was the case at all pH values. With regard to the PS and PMMA domains, the changes in site preference with pH are interpreted in terms of changes in the proportions of exposed hydrophobic and hydrophilic residues of albumin, which in turn are related to conformational changes of the albumin. Interestingly, when albumin is in its naturally compact (pH 7.0), completely extended (pH 2.0), and completely contracted (pH 10.0) structures, it has an adsorption preference similar to that of the PS and PMMA regions, indicating the surfaces of these "equilibrium" structures have similar proportions of hydrophobic



and hydrophilic residues. However, in the intermediate stages of extending (pH 4.0) or contracting (pH 8.6), the albumin surface is quite different. When it is extending, albumin opens up some hydrophilic crevices, as indicated by the preferential adsorption of albumin on the relatively hydrophilic PMMA domains at pH 4.0. In contrast, the albumin surface hides hydrophilic residues when contracting, as indicated by preferential adsorption of albumin on the more hydrophobic PS domains at pH 8.6.

**Acknowledgment.** This research is supported by the Natural Sciences and Engineering Research Council (NSERC, Canada), The Canadian Foundation for Innovation, and the Canada Research Chair program. X-ray microscopy was carried out using PEEM2 at the ALS. The ALS is supported by the Office of Basic Energy Sciences of the U.S. Department of Energy under contract DE-AC03-76SF00098.

## References and Notes

- (1) Peters, T., Jr. *All About Albumin: Biochemistry, Genetics, and Medical Applications*; Academic Press: New York, 1995.
- (2) Foster, J. F. In *Albumin Structure, Function and Uses*; Rosenoer, V. M., Oratz, M., Rothschild, M. A., Eds.; Pergamon: Oxford, 1977; pp 53–84.
- (3) Carter, D. C.; Ho, J. X. *Adv. Protein Chem.* **1994**, *45*, 153–203.
- (4) Qiu, W.; Zhang, L.; Okobiah, L.; Yang, Y.; Wang, L.; Zhong, D.; Zewail, A. H. *J. Phys. Chem. B* **2006**, *110*, 10540–10549.
- (5) Morin, C.; Ikeura-Sekiguchi, H.; Tylistczak, T.; Cornelius, R.; Brash, J. L.; Hitchcock, A. P.; Scholl, A.; Nolting, F.; Appel, G.; Winesett, A. D.; Kaznacheyev, K.; Ade, H. *J. Electron Spectrosc.* **2001**, *121*, 203–224.
- (6) Morin, C.; Hitchcock, A. P.; Cornelius, R. M.; Brash, J. L.; Scholl, A.; Doran, A. *J. Electron Spectrosc.* **2004**, *137–140*, 785–794.
- (7) Li, L.; Hitchcock, A. P.; Robar, N.; Cornelius, R.; Brash, J. L.; Scholl, A.; Doran, A. *J. Phys. Chem. B* **2006**, *110*, 16763–16773.
- (8) Sousa, A.; Sengonul, M.; Latour, R.; Kohn, J.; Libera, M. *Langmuir* **2006**, *22*, 6286–6292.
- (9) Rapoza, R. J.; Horbett, T. A. *J. Biomed. Mater. Res.* **1990**, *24*, 1263–1287.
- (10) Pierce Chemical Company, IODO-GEN Iodination Reagent, 1993.
- (11) Regoeczi, E. *Iodine-Labeled Plasma Proteins*; CRC Press: Boca Raton, FL, 1984; Vol. 1.
- (12) Chan, B. M. C.; Brash, J. L. *J. Colloid Interface Sci.* **1981**, *82*, 217–225.
- (13) Anders, S.; Padmore, H. A.; Duarte, R. M.; Renner, T.; Stammer, T.; Scholl, A.; Scheinfein, M. R.; Stöhr, J.; Séve, L.; Sinkovic, B. *Rev. Sci. Instrum.* **1999**, *70*, 3973–3981.
- (14) Jacobsen, C.; Wirick, S.; Flynn, G.; Zimba, C. *J. Microsc.* **2000**, *197*, 173–184.
- (15) van der Veen, M.; Norde, W.; Stuart, M. C. *Colloids Surf., B: Biointerfaces* **2004**, *35*, 33–40.
- (16) Salim, M.; O'Sullivan, B.; McArthur, S. L.; Wright, P. C. *Lab Chip* **2007**, *7*, 64–70.
- (17) Hitchcock, A. P.; Morin, C.; Zhang, X.; Araki, T.; Dynes, J. J.; Stöver, H.; Brash, J. L.; Lawrence, J. R.; Leppard, G. G. *J. Electron Spectrosc. Relat. Phenom.* **2005**, *259–269*, 144–147.
- (18) Wang, J.; Morin, C.; Li, L.; Hitchcock, A. P.; Doran, A.; Scholl, A. *J. Electron Spectrosc.*, in press.
- (19) Hitchcock, A. P.; Morin, C.; Heng, Y. M.; Cornelius, R. M.; Brash, J. L. *J. Biomater. Sci., Polymer Ed.* **2002**, *13*, 919–938.
- (20) Kadi, N. E. I.; Taulier, N.; Le Huérou, J. Y.; Gindre, M.; Urbach, W.; Nwigwe, I.; Kahn, P. C.; Waks, M. *Biophys. J.* **2006**, *91*, 3397–3404.
- (21) Carter, D. C.; He, X. M.; Munson, S. H.; Twigg, P. D.; Gernert, K. M.; Broom, M. B.; Miller, T. Y. *Science* **1989**, *244*, 1195–1198.
- (22) Sugio, S.; Kashima, A.; Mochizuki, S.; Noda, M.; Kobayashi, K. *Protein Eng.* **1999**, *12*, 439–446.
- (23) Hughes, W. L. In *The Proteins*; Neurath, H., Biley, K., Eds.; Academic Press: New York, 1954; Vol. 2b, pp 663–755.
- (24) Squire, P. G.; Moser, P.; O'Konski, C. T. *Biochemistry* **1968**, *7*, 4261–4272.
- (25) Wright, A. K.; Thompson, M. R. *Biophys. J.* **1975**, *15*, 137–141.
- (26) Bloomfield, V. *Biochemistry* **1966**, *5*, 684–689.
- (27) Ferrer, M. L.; Duchowicz, R.; Carrasco, B.; Torre, J. G.; Acuña, A. U. *Biophys. J.* **2001**, *2422–2430*.
- (28) Guinier, A.; Fournet, G. *Small-Angle Scattering of X-rays*; J. Wiley and Sons: New York, 1955.
- (29) Harrubgtoon, W. F.; Johnson, P.; Ottewill, R. H. *Biochem. J.* **1956**, *62*, 569–582.
- (30) Olivieri, J. R.; Craievich, A. F. *Eur. Biophys. J.* **1995**, *24*, 77–84.
- (31) Green, R. J.; Davies, J.; Davies, M. C.; Robert, C. J.; Tendler, S. J. B. *Biomaterials* **1997**, *18*, 405–413.
- (32) Peters, T., Jr. *All About Albumin: Biochemistry, Genetics, and Medical Applications*; Academic Press: New York, 1995.
- (33) Alizadeh-Pasdar, N.; Li-Chan, E. C. Y. *J. Agric. Food Chem.* **2000**, *48*, 328–334.